Ferromagnetic Carbodiimide

DOI: 10.1002/anie.201000387

A Ferromagnetic Carbodiimide: $Cr_2(NCN)_3$**

*Xiaojuan Tang, Hongping Xiang, Xiaohui Liu, Manfred Speldrich, and Richard Dronskowski**

Extended pseudochalcogenides such as the solid-state carbodiimides (incorporating complex $^{-}N{=}C{=}N^{-}$ units with $D_{\infty h}$ symmetry) or cyanamides (with a less symmetrical $N{\equiv}C{-}N^{2-}$ unit) have been extensively investigated, and a large number including alkali[1] and alkaline-earth metals,[2] main-group elements,[3] d^{10} transition metals,[4] and also rare-earth metals[5] have been reported. The synthesis of the complete set of *M*NCN (*M* = Mn–Cu) phases with only partially filled 3d orbitals, however, looked far more difficult, because first-principles calculations[6] had predicted them to be unstable in terms of formation enthalpy ΔH_f and Gibbs formation energy ΔG_f, with the instability continuously rising from MnNCN to CuNCN, thereby mirroring the gradual filling of antibonding levels from $3d^5$ to $3d^9$.

Nonetheless, we have succeeded in finding new routes to synthesize the *M*NCN series of the divalent 3d metals as a prerequisite to determine their crystal structures. MnNCN, the first carbodiimide of a magnetic transition metal ever realized, is made by a metathesis around 600 °C involving ZnNCN and $MnCl_2$[7] but this method is unsuitable for the later, more unstable compounds. FeNCN,[8] CoNCN, and NiNCN[9] are synthesized, instead, by a two-step route via the corresponding hydrogencyanamides $M(HNCN)_2$ at about 400 °C.[10] Finally, the most delicate carbodiimide, CuNCN, is obtained by the oxidation of a copper(I) cyanamide precursor under aqueous conditions at room temperature.[11]

The magnetic properties of the carbodiimides involving divalent transition metals are similar to those of the isolobal oxides, in particular by indicating antiferromagnetic interactions. For example, the magnetic structure of MnNCN based on spin-polarized neutron diffraction reveals frustration between the high-spin ($S = 5/2$) Mn^{2+} ions as a function of temperature[12] but also shows that the carbodiimide unit ensures a strong magnetic communication. Likewise, experimental as well as theoretical studies on the magnetic structure of CuNCN have shown a fascinating interplay between geometrical packing and exchange couplings.[13] Finally, UV/Vis measurements on MnNCN[14] stress the importance of the more covalent Mn–N bond and higher ligand-field splitting compared to Mn–O chromophores but a smaller nephelauxetic ratio. Also, the Mn–N bond lacks significant π interaction.

[*] X. Tang, Dr. H. Xiang, Dr. X. Liu, Dr. M. Speldrich, Prof. Dr. R. Dronskowski
Institute of Inorganic Chemistry, RWTH Aachen University
Landoltweg 1, 52056 Aachen (Germany)
Fax: (+49) 241-80-92642
E-mail: drons@HAL9000.ac.rwth-aachen.de
Homepage: www.ssc.rwth-aachen.de

[**] The authors acknowledge the financial support by the German Science Foundation (DFG). We would also like to thank Dipl.-Ing. Ludwig Stork for chemical assistance.

In light of this information, the design of a carbodiimide that is not antiferromagnetic requires an alternative composition, for example, by moving towards a different oxidation state. The hypothetical chromium(III) carbodiimide, $Cr_2(NCN)_3$, is such a synthetic target although its isolobal oxide Cr_2O_3 is, in fact, antiferromagnetic. Because the electron configuration ($3d^3$) is even lower than in the MnNCN case, theory[6] implies that the synthetic route for MnNCN should also be applicable for $Cr_2(NCN)_3$. In addition, there is related information with respect to existing rare-earth metal(III) carbodiimides. Recent research on such $Ln_2(NCN)_3$ phases by others[5d,e] provided similar layer structures to those of the *M*NCN phases but with different coordination modes. The changes in coordination mode must result in different magnetic exchange couplings, and that is what we were looking for.

We have now synthesized green $Cr_2(NCN)_3$, the first transition-metal(III) carbodiimide with a $3d^3$ configuration, by a metathesis between $CrCl_3$ and freshly made ZnNCN. The compound appears to be highly inert. Not too surprisingly, the structural determination yields that $Cr_2(NCN)_3$ is isostructural with $Yb_2(NCN)_3$.[5e] It is astounding, however, that $Cr_2(NCN)_3$ indeed shows ferromagnetic properties, in contrast to all other transition-metal carbodiimides. We also reiterate the fact that $Cr_2(NCN)_3$ is very similar to the related oxide Cr_2O_3 crystallographically but not in terms of magnetism.

As alluded to already, high-resolution X-ray powder diffraction (XRPD) demonstrates that $Cr_2(NCN)_3$ can be synthesized in phase-pure form and that it crystallizes in the rhombohedral space group $R\bar{3}c$. As a result of the very good crystallinity, the structure refinement could be based on the well-resolved data shown in Figure 1.

The crystal structure of chromium(III) carbodiimide as well as the coordination environments of both the Cr^{3+} and NCN^{2-} ions are displayed in Figure 2. The packing corresponds to a formally layered structure with each layer consisting of alternating Cr^{3+} and NCN^{2-} ions along the *c* axis (Figure 2; left), similar to the transition-metal(II) carbodiimides.

Nonetheless, the packing of the metal layers is not dense because each metal atom is surrounded by only three, not six neighboring metal atoms. The chromium coordination (Figure 2; right) corresponds to a slightly distorted N_6 octahedron with practically identical bond lengths (Cr–N 2.081(5) and 2.101(4) Å, three of each), and these agree well with the sum of the effective ionic radii (2.08 Å).[15] The 2:3 stoichiometric ratio ensures that each N atom bonds only to two Cr, analogous to the corundum-type structure of Cr_2O_3.[16] The NCN^{2-} ion, which is practically linear (N-C-N 178.0(7)°), experiences a distorted tetrahedral coordination by the Cr ions, and it almost coincides with the *c* axis. Thus, this unit

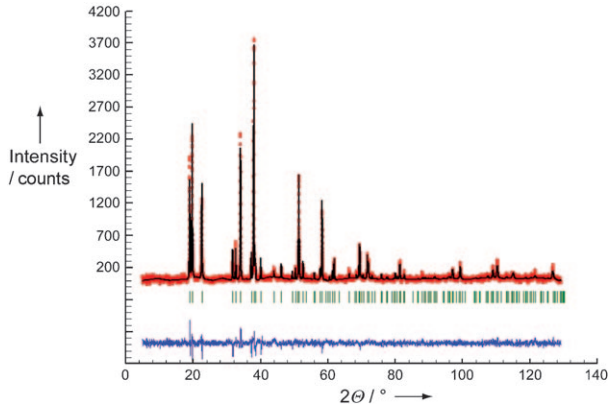

Figure 1. Observed, calculated, and difference intensities of the X-ray Rietveld refinement of $Cr_2(NCN)_3$ using Cu-Kα_1 radiation. The vertical positions of the Bragg reflections are given in green.

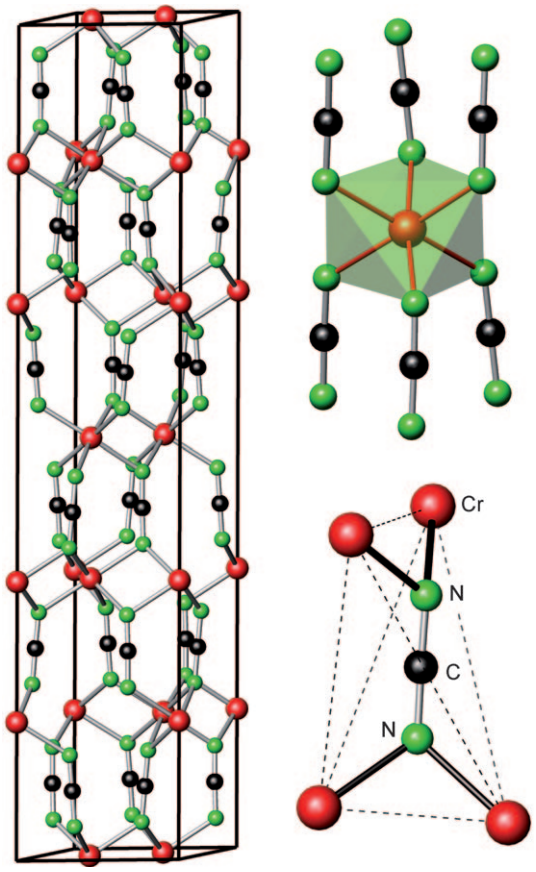

Figure 2. Crystal structure of $Cr_2(NCN)_3$ (left) and the coordination environments of the Cr^{3+} ion and the NCN^{2-} ion (right).

adopts the symmetrical carbodiimide shape with C–N 1.208(4) Å, and this can also be verified by the IR spectrum of $Cr_2(NCN)_3$, which shows asymmetric stretching vibrations of the NCN^{2-} unit at $\nu_{as} = 2005$ and 2094 cm^{-1} together with the deformation vibrations δ at 635 and 696 cm^{-1}.

The magnetic susceptibility data of $Cr_2(NCN)_3$ were determined at applied fields B_0 between 0.01 and 0.5 T in the temperature range between 2 and 400 K. Figure 3 displays a plot of the (inverse) molar susceptibility as a function of T and the magnetic hysteretic loop at fields up to 5 T at $T = 10$ K

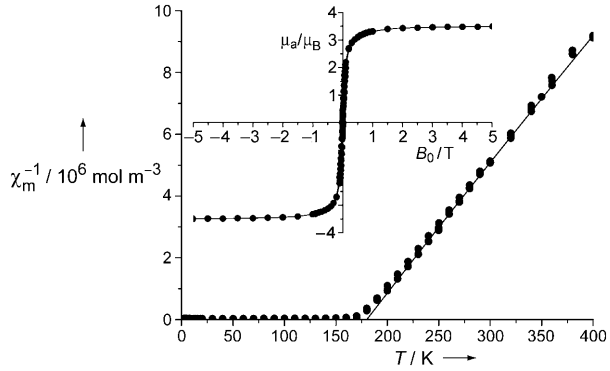

Figure 3. Inverse molar magnetic susceptibility versus temperature plot for $Cr_2(NCN)_3$ in SI units at applied fields of $B_0 = 0.01$, 0.1, and 0.5 T (experimental data dotted, fitted data as a solid line; see text for parameter values). Insert: magnetic hysteretic loop with fields up to 5 T at a temperature of 10 K.

(Figure 3; insert). Chromium(III) carbodiimide displays a hysteretic magnetization with a coercivity H_c of about 0.01 T (100 Oe) and a saturation magnetization of close to 3.5 μ_B which equals a specific magnetization of $\sigma = 86$ A m^2 kg^{-1}. The small coercivity is typical for a magnetically soft material.

The χ_m^{-1} versus T plot manifests a linear range between 200–400 K with a positive paramagnetic Curie temperature θ. Consequently, a linear fit to the Curie–Weiss law beyond 200 K leads to $C = 2.071 \times 10^{-5}$ m^3 K mol^{-1} and a θ value equal to 178 K (Figure 3).

We note that the experimentally derived paramagnetic moment, on the basis of this C value, equals 3.6 μ_B which is very close to an ideal octahedral $3d^3$ high-spin system (Cr^{3+}, ligand-field ground state $^4A_2$, three unpaired electrons, $S = 3/2$, $\mu_{so} = g[S(S+1)]^{1/2} = 3.87\,\mu_B$ with $g \approx 2$).[17] For a deeper analysis, the magnetic properties were further modeled by using the Hamiltonian [Eq. (1)]

$$\hat{H} = H_{ee} + H_{lf} + H_{so} + H_{ex} + H_{mag} \quad (1)$$

which includes the effects of the interelectronic repulsion (H_{ee}), ligand-field (H_{lf}), spin-orbit coupling (H_{so}), exchange interactions (H_{ex}), and the applied field (H_{mag}). The exchange interactions between the magnetic Cr^{3+} ions are described by the molecular-field approximation [Eq. (2)]

$$\chi_m^{-1} = \chi_m'^{-1}\left(B, C, \zeta, B_q^k\right) - \lambda_{mf} \quad (2)$$

where λ_{mf} is the molecular-field parameter and χ_m' the susceptibility per isolated Cr^{3+} ion. The molecular-field parameter causes a parallel shift of the χ_m^{-1} versus T plot in the case of pure-spin ions [Eq. (3)].

$$\chi_m^{-1} = \frac{T}{C} - \lambda_{mf} \Rightarrow \chi_m = \frac{C}{T-\theta} \quad \text{with } \theta = \lambda_{mf} C \quad (3)$$

The molecular field is the source of the difference between an ion's local effective magnetic field and the applied magnetic field. A positive (or negative) λ_{mf} indicates predominantly ferromagnetic (or antiferromagnetic) interactions, respectively. The ligand-field effect, spin-orbit coupling, interelectronic repulsion, as well as exchange coupling were taken into account using a spin-orbit coupling constant $\zeta = 273\ cm^{-1}$ and Racah parameters of $B = 1030\ cm^{-1}$ and $C = 3680\ cm^{-1}$ as derived from optical spectra.[18] Then, the analysis with the help of CONDON[19] employed a ligand-field parameter B_0^4 whose starting value was based on the GGA + U calculations (see below). The best fit arrived at $B_0^4 = -16050\ cm^{-1}$, $\lambda_{mf} = 8.589 \times 10^7\ mol\,m^{-3}$, and SQ = 1.3 %, where B_q^k refers to the Wybourne notations[20] of the ligand-field parameters and $SQ = \Sigma[(\chi_{obs} - \chi_{cal})/(\chi_{obs})]^2$ quantifies the fit quality. The size of λ_{mf} corresponding to $\theta = 178$ K for a ligand-field ground term $^4A_2$ suggests very strong exchange interactions, and the positive signs of both θ and λ_{mf} indicate dominantly ferromagnetic interactions. Indeed, a magnetochemical CONDON analysis provides a satisfactory fit only if ferromagnetic interactions are considered.

Alternating-current (AC) magnetization data of $Cr_2(NCN)_3$ were collected with an oscillating field of 3 Oe at three different frequencies (10, 100, 500 Hz). Figure 4 (top) displays the in-phase magnetization (m') versus T and also the out-of-phase magnetization (m'', Figure 4, bottom). The presence of a frequency-dependent out-of-phase signal in the AC susceptibility for $T = 130$–210 K is indicative of a magnetization relaxation relative to the frequency of the oscillating field, thereby corroborating the ferromagnetic ordering. We conclude that the experimental data can be modeled by a set of ligand-field parameters which are in line with GGA + U calculations (see below), and λ_{mf} as well as the frequency-dependent out-of-phase AC signal support ferromagnetism below 180 K. In comparison to typical ferromagnetic oxides, such as CrO_2 and, in particular, ferrimagnetic γ-Fe_2O_3 ($\sigma = 80\ A\,m^2\,kg^{-1}$), $Cr_2(NCN)_3$ has a slightly larger specific magnetization but at lower temperatures; in addition, its coercivity is much lower.[21]

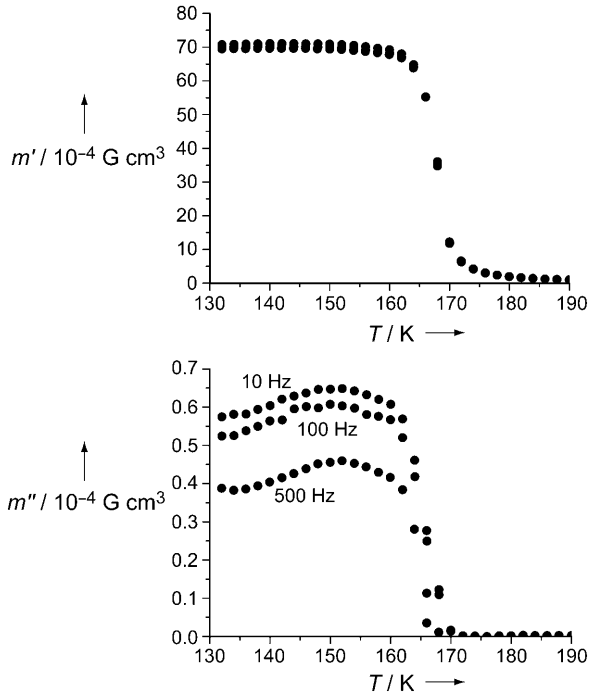

Figure 4. In-phase AC magnetization m' versus temperature plot of $Cr_2(NCN)_3$ (top) and out-of-phase AC magnetization m'' versus temperature (bottom). The data were collected in a 3 Oe oscillating magnetic field for the frequencies 10, 100, and 500 Hz.

To achieve quantum-chemical insight into the magnetic properties and exchange couplings, we also performed first-principles electronic-structure calculations of density-functional type based on the generalized-gradient approximation (GGA)[22] and the projector-augmented wave method.[23] In addition, explicit electron–electron Coulomb interactions plus the self-interaction correction were considered in the rotationally invariant way (GGA + U)[24] with one effective Hubbard parameter $U_{eff} = U - J$, in which U_{eff} is equal to 4 eV as has been successfully applied in the case of Cr_2O_3.[25]

Besides the simple ferromagnetic (FM) structure with all the magnetic moments of chromium pointing in the same direction, three additional antiferromagnetic structures were chosen in which the four neighboring Cr^{3+} ions A, B, C, D along the [111] axis (Figure 5) adopt different orientations with respect to their local moments.

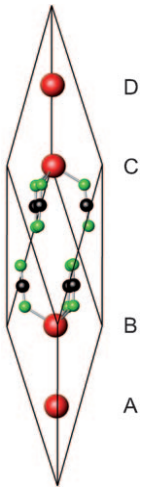

Figure 5. The primitive trigonal unit cell of the $Cr_2(NCN)_3$ crystal structure containing four Cr^{3+} ions (red) and six NCN^{2-} ions (green and black). The labels A, B, C, and D refer to different magnetic orientations of the local chromium moment.

If the symbols + and − stand, respectively, for a spin-up and spin-down orientation of a Cr moment, then the sequence + + + + represents the ferromagnetic case, + − + − is the AFM1 model (adopted by Cr_2O_3),[26] + + − − is the AFM2 model (adopted by α-Fe_2O_3),[27] while + − − + is the AFM3 model (no representative to date). In the GGA context, the total energy of the FM state is the same as that of the AFM1 state, and both are lower than AFM2 and AFM3 by 26 meV and 124 meV per formula unit, respectively. Within GGA + U theory, however, the FM state is clearly the most stable one, lower than AFM1, AFM2, and AFM3, by about 29 meV,

50 meV, and 82 meV, respectively. Thus, GGA + U theory also mirrors the experimental finding of $Cr_2(NCN)_3$ being ferromagnetic, in contrast to the isostructural but antiferromagnetic phases Cr_2O_3 and α-Fe_2O_3. The calculated spin saturation moments for the Cr^{3+} ion are 2.88 μ_B and 3.08 μ_B for GGA and GGA + U theory, respectively, in very good agreement (GGA + U) with the $S = 3/2$ scenario and the experimental paramagnetic moment of 3.6 μ_B.

The local densities-of-states (DOS) within the FM state as derived from GGA and GGA + U theory are shown in Figure 6. In the GGA description, the Cr–N orbital mixing is

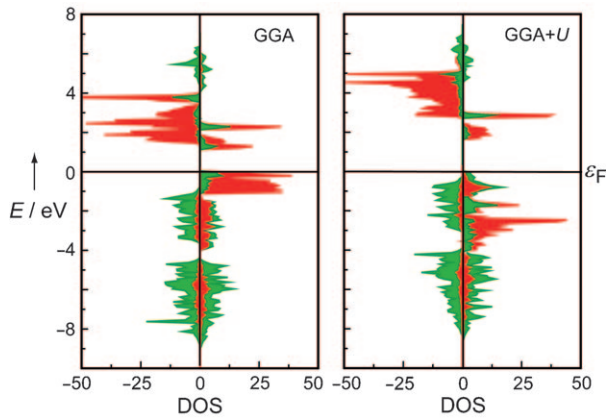

Figure 6. The local densities-of-states (DOS) of the Cr 3d (red) and N 2p (green) orbitals of $Cr_2(NCN)_3$ in the ferromagnetic state as modeled from GGA (left) and GGA + U (right) calculations, with the spin-up and spin-down electrons given to the right and left in each frame. The energy zero indicates the Fermi level.

astonishingly weak, and the energy gap of about 1.2 eV is between the highest occupied majority valence bands with Cr t_{2g} character and the lowest-lying conduction bands of mixed character (majority Cr e_g, minority Cr t_{2g}) thereby classifying $Cr_2(NCN)_3$ as a d–d Mott–Hubbard insulator. Upon including an on-site Coulomb interaction (GGA + U), the occupied Cr 3d states shift to even lower energies which immediately translates into an increased mixing between the Cr 3d and the N 2p orbitals. The somewhat larger energy gap (1.7 eV) is now found between the highest valence band of strongly mixed Cr t_{2g} and N 2p character and the lowest conduction band of Cr e_g character. In short, the electronic structures of $Cr_2(NCN)_3$ both from GGA and GGA + U are similar to those of Cr_2O_3 which is typically considered as an intermediate between a charge-transfer (CT) and a Mott–Hubbard (MH) insulator, both from the experimental[28] and also the theoretical[29] perspective. Hence, we conclude that $Cr_2(NCN)_3$ is also a ferromagnetic intermediate CT–MH insulator, in good accord with the macroscopic appearance of a green ferromagnetic material.

In summary, we have synthesized the first transition-metal(III) carbodiimide, $Cr_2(NCN)_3$, in phase-pure form and determined its crystal structure and magnetic properties. $Cr_2(NCN)_3$ is an astonishingly inert material which adopts the same crystal structure as the related antiferromagnet Cr_2O_3; nonetheless, both experiment and GGA + U electronic-structure theory clearly indicate that $Cr_2(NCN)_3$ is ferromagnetic. We consider these results an important step for finding novel types of magnetic materials.

Experimental Section

All synthetic steps were carried out in an argon-filled glove box. The reaction mixture comprises $CrCl_3$ (99.9 %, Alfa) and freshly prepared ZnNCN, in slightly above the ideal 2:3 molar ratio together with a mixture of LiCl/KCl (46:54, m.p. = 352 °C) needed as a flux. Both reactants and flux were heated at 300 °C under dynamic vacuum for 12 h and then to 550 °C for another two days. The reaction follows the simplest equation: $2\,CrCl_3 + 3\,ZnNCN \rightarrow Cr_2(NCN)_3 + 3\,ZnCl_2$. The resulting powder was washed using dilute HCl, water. and acetone. Green $Cr_2(NCN)_3$ is not only inert against air and water, but also against acidic and alkaline conditions (!) over the entire pH range between 1 and 14.

The high-resolution powder XRD pattern was collected with a Stoe STADI MP powder diffractometer in transmission geometry with strictly monochromatized Cu-Kα_1 radiation, a linear position-sensitive detector, and a flat-sample holder. The WinXPOW program[30] was used for indexing the data. The primary structural model was deduced by comparison with the crystal structure of $Yb_2(NCN)_3$. The Rietveld refinement on the basis of a pseudo-Voigt profile function was carried out by using the Fullprof program package.[31]

Crystal data of $Cr_2(NCN)_3$: $M_r = 224.06$, space group $R\bar{3}c$ (no. 167); $a = b = 5.4751(1)$ Å, $c = 27.9696(3)$ Å, $V = 726.10(2)$ Å^3, $Z = 6$; $R_p = 0.017$; $R_{wp} = 0.024$; $R_{Bragg} = 0.096$; Cr on 12c with $z = 0.1659(1)$; C on 18e with $x = 0.3166(11)$ and N on 36f with $x = 0.6416(7)$, $y = 0.0004(8)$ and $z = 0.0404(1)$. Further details on the crystal structure investigations may be obtained from the Fachinformationszentrum Karlsruhe, 76344 Eggenstein-Leopoldshafen, Germany (fax: (+49) 7247-808-666; e-mail: crysdata@fiz-karlsruhe.de), on quoting the depository number CSD-421391 for $Cr_2(NCN)_3$.

Infrared data were measured with a Nicolet Avatar 360 FT-IR E.S.P. spectrophotometer in a range from 400 to 4000 cm^{-1} with KBr disks: $\nu_{as}(NCN) = 2005/2094$ cm^{-1}, $\delta(NCN) = 635/696$ cm^{-1}.

Magnetic susceptibility measurements were carried out by SQUID magnetometry (MPMS-5S, Quantum Design, San Diego, CA) in the temperature range between 2–400 K and at applied fields B_0 between 0.01–5 T. The data were corrected for the sample holder (Teflon tubes) and the diamagnetic contributions of Cr^{3+} ions and the carbodiimide ligand (approximately $\chi_m = -14.1 \times 10^{-10}$ m^3 mol^{-1}).

The periodic density-functional theory calculations were performed with the Vienna ab initio simulation package (VASP).[32]

Received: January 22, 2010
Published online: May 31, 2010

Keywords: carbodiimides · chromium · magnetic properties · Rietveld refinement

[1] a) M. G. Down, M. J. Haley, P. Hubberstey, R. J. Pulham, A. E. Thunder, *J. Chem. Soc. Dalton Trans.* **1978**, 1407–1411; b) A. Harper, P. Hubberstey, *J. Chem. Res. Synop.* **1989**, *7*, 194–195; c) M. Becker, J. Nuss, M. Jansen, *Z. Anorg. Allg. Chem.* **2000**, *626*, 2505–2508; d) W. Schnick, H. Huppertz, *Z. Anorg. Allg. Chem.* **1995**, *621*, 1703–1707; e) M. Becker, M. Jansen, *Z. Naturforsch. B* **1999**, *54*, 1375–1378.

[2] a) N.-G. Vannerberg, *Acta Chem. Scand.* **1962**, *16*, 2263–2266; b) U. Berger, W. Schnick, *J. Alloys Compd.* **1994**, *206*, 179–184; c) O. Reckeweg, F. J. DiSalvo, *Angew. Chem.* **2000**, *112*, 397–399; *Angew. Chem. Int. Ed.* **2000**, *39*, 412–414; d) W. Liao, R. Dronskowski, *Acta Crystallogr. Sect. E* **2004**, *60*, 124–126.

[3] a) R. Dronskowski, *Z. Naturforsch. B* **1995**, *50*, 1245 – 1251; b) R. Riedel, A. Greiner, G. Miehe, W. Dreßler, H. Fueß, J. Bill, F. Aldinger, *Angew. Chem.* **1997**, *109*, 657 – 660; *Angew. Chem. Int. Ed. Engl.* **1997**, *36*, 603 – 606; c) M. J. Cooper, *Acta Crystallogr.* **1964**, *17*, 1452 – 1456; d) X. Liu, A. Decker, D. Schmitz, R. Dronskowski, *Z. Anorg. Allg. Chem.* **2000**, *626*, 103 – 105; e) L. Stork, X. Liu, B. P. T. Fokwa, R. Dronskowski, *Z. Anorg. Allg. Chem.* **2007**, *633*, 1339 – 1342.

[4] a) F. P. Bowden, H. M. Montagu-Pollock, *Nature* **1961**, *191*, 556 – 558; b) M. Becker, J. Nuss, M. Jansen, *Z. Naturforsch. B* **2000**, *55*, 383 – 385; c) M. Becker, M. Jansen, *Acta Crystallogr. Sect. C* **2001**, *57*, 347 – 348; d) G. Baldinozzi, B. Malinowska, M. Rakib, G. Durand, *J. Mater. Chem.* **2002**, *12*, 268 – 272; e) M. Becker, M. Jansen, *Z. Anorg. Allg. Chem.* **2000**, *626*, 1639 – 1641; f) X. Liu, P. Müller, P. Kroll, R. Dronskowski, *Inorg. Chem.* **2002**, *41*, 4259 – 4265; g) X. Liu, P. Müller, R. Dronskowski, *Z. Anorg. Allg. Chem.* **2005**, *631*, 1071 – 1074.

[5] a) O. Reckeweg, F. J. DiSalvo, *Z. Anorg. Allg. Chem.* **2003**, *629*, 177 – 179; b) R. Srinivasan, M. Stöbele, H.-J. Meyer, *Inorg. Chem.* **2003**, *42*, 3406 – 3411; c) W. Liao, C. Hu, R. K. Kremer, R. Dronskowski, *Inorg. Chem.* **2004**, *43*, 5884 – 5890; d) M. Neukirch, S. Tragl, H.-J. Meyer, *Inorg. Chem.* **2006**, *45*, 8188 – 8193; e) O. Reckeweg, T. Schleid, F. J. DiSalvo, *Z. Naturforsch. B* **2007**, *62*, 658 – 662.

[6] M. Launay, R. Dronskowski, *Z. Naturforsch. B* **2005**, *60*, 437 – 448.

[7] X. Liu, M. Krott, P. Müller, C. Hu, H. Lueken, R. Dronskowski, *Inorg. Chem.* **2005**, *44*, 3001 – 3003.

[8] X. Liu, L. Stork, M. Speldrich, H. Lueken, R. Dronskowski, *Chem. Eur. J.* **2009**, *15*, 1558 – 1561.

[9] M. Krott, X. Liu, B. P. T. Fokwa, M. Speldrich, H. Lueken, R. Dronskowski, *Inorg. Chem.* **2007**, *46*, 2204 – 2207.

[10] M. Krott, X. Liu, P. Müller, R. Dronskowski, *J. Solid State Chem.* **2007**, *180*, 307 – 312.

[11] X. Liu, M. A. Wankeu, H. Lueken, R. Dronskowski, *Z. Naturforsch. B* **2005**, *60*, 593 – 596.

[12] M. Krott, A. Houben, P. Müller, W. Schweika, R. Dronskowski, *Phys. Rev. B* **2009**, *80*, 024117.

[13] a) X. Liu, R. Dronskowski, R. K. Kremer, M. Ahrens, C. Lee, M.-H. Whangbo, *J. Phys. Chem. C* **2008**, *112*, 11013 – 11017; b) H. Xiang, X. Liu, R. Dronskowski, *J. Phys. Chem. C* **2009**, *113*, 18891 – 18896; c) A. A. Tsirlin, H. Rosner, *Phys. Rev. B* **2010**, *81*, 024424.

[14] X. Liu, R. Dronskowski, R. Glaum, A. Tchougréeff, *Z. Anorg. Allg. Chem.* **2010**, *636*, 343 – 348.

[15] R. D. Shannon, *Acta Crystallogr. Sect. A* **1976**, *32*, 751 – 767.

[16] O. Madelung, U. Rössler, M. Schulz (Eds.), *Non-Tetrahedrally Bonded Binary Compounds II*, *Vol. 41D*, Springer, Berlin, **2000**.

[17] H. Lueken, *Magnetochemie*, Teubner, Stuttgart **1999**.

[18] J. S. Griffith, *The Theory of Transition-Metal Ions*, Cambridge University Press, Cambridge, **1964**.

[19] H. Schilder, H. Lueken, *J. Magn. Magn. Mater.* **2004**, *281*, 17 – 26.

[20] B. G. Wybourne, *Spectroscopic Properties of Rare Earths*, Wiley, New York, **1965**.

[21] S. Chikazumi, *Physics of Ferromagnetism*, 2nd. ed., Clarendon Press, Oxford, **1997**.

[22] J. P. Perdew, K. Burke, M. Ernzerhof, *Phys. Rev. Lett.* **1996**, *77*, 3865 – 3868.

[23] a) P. E. Blöchl, *Phys. Rev. B* **1994**, *50*, 17953 – 17979; b) G. Kresse, D. Joubert, *Phys. Rev. B* **1999**, *59*, 1758 – 1775.

[24] a) V. I. Anisimov, F. Aryasetiawan, A. I. Liechtenstein, *J. Phys. Condens. Matter* **1997**, *9*, 767 – 808; b) S. L. Dudarev, G. A. Botton, S. Y. Savrasov, C. J. Humphreys, A. P. Sutton, *Phys. Rev. B* **1998**, *57*, 1505 – 1509.

[25] N. J. Mosey, E. A. Carter, *Phys. Rev. B* **2007**, *76*, 155123.

[26] T. R. McGuire, E. J. Scott, F. H. Grannis, *Phys. Rev.* **1956**, *102*, 1000 – 1003.

[27] C. G. Shull, W. A. Strauser, E. O. Wollan, *Phys. Rev.* **1951**, *83*, 333 – 345.

[28] T. Uozumi, K. Okada, A. Kotani, R. Zimmermann, P. Steiner, S. Hüfner, Y. Tezuka, S. Shin, *J. Electron Spectrosc. Relat. Phenom.* **1997**, *83*, 9 – 20.

[29] A. Rohrbach, J. Hafner, G. Kresse, *Phys. Rev. B* **2004**, *70*, 125426.

[30] WinXPOW, Version 1.06. STOE & CIE GmbH, **1999**.

[31] J. Rodriguez-Carvajal, Fullprof2000, Version 3.2, Laboratoire Léon Brillouin, **1997**.

[32] a) G. Kresse, J. Furthmüller, *Comput. Mater. Sci.* **1996**, *6*, 15 – 50; b) G. Kresse, J. Furthmüller, *Phys. Rev. B* **1996**, *54*, 11169 – 11186; c) G. Kresse, J. Hafner, *Phys. Rev. B* **1993**, *47*, 558 – 561; d) G. Kresse, J. Hafner, *Phys. Rev. B* **1994**, *49*, 14251 – 14269.

